Fitoterapia 138 (2019) 104288

Contents lists available at ScienceDirect

Fitoterapia

journal homepage: www.elsevier.com/locate/fitote

Sesquiterpenoids and γ-pyranone derivatives from the whole plant of *Erigeron breviscapus* and their neuroprotective effects

Shuang Han[a], Ying Liu[a], Zilin Hou[a], Xiujia Sun[c], Guodong Yao[a], Pinyi Gao[a,b,*], Lingzhi Li[a,*], Shaojiang Song[a,**]

[a] School of Traditional Chinese Materia Medica, Key Laboratory of Computational Chemistry-Based Natural Antitumor Drug Research & Development, Liaoning Province, Shenyang Pharmaceutical University, Shenyang 110016, People's Republic of China
[b] College of Pharmaceutical and Biotechnology Engineering, Institute of Functional Molecules, Shenyang University of Chemical Technology, 11 Street, Shenyang economic and Technological Development Zone, Shenyang 110142, People's Republic of China
[c] Shanghai Key Laboratory of Psychotic Disorders, Shanghai Mental Health Center, Shanghai Jiao Tong University School of Medicine, Shanghai, 200030, People's Republic of China

ARTICLE INFO

Keywords:
Erigeron breviscapus
Sesquiterpene
ECD calculation
Optical rotation calculation
Neuroprotective effect

ABSTRACT

Four new sesquiterpenes (**1–2**, **6–7**), a new pyranone glycoside (**10**) along with six known compounds, were isolated from the whole plant of *Erigeron breviscapus*. Their planar structures were elucidated using extensive spectroscopic analyses. Brevisterpene A (**1**) and brevisterpene B (**2**) were proved to be a pair of diastereomer followed by mixtures resolution using chiral HPLC. Their absolute configurations were determined by ECD calculation. The relative configuration of brevisnoside B (**7**) was elucidated by a combined analysis of NOESY spectrum and computation of ^{13}C NMR chemical shifts, and determination of the absolute configurations of **6** and **7** assisted by optical rotation calculations. Compounds **1** and **2** displayed moderate neuroprotective effects against H_2O_2-induced damage in SH-SY5Y cells.

1. Introduction

Erigeron breviscapus (Vaniot) Hand.-Mazz., a traditional Chinese herb medicine, is a perennial, clump-forming shrub belonging to the Compositae family, widely distributed throughout southwest China [1,2]. The dried whole plant of *E. breviscapus* is used for the treatment of cerebrovascular disease, coronary heart disease, cerebral embolism, paralysis caused by cerebral vascular accidents, and apoplexy [3–5]. Previous studies revealed that *E. breviscapus* possessed multiple bioactivities including antioxidant, anti-inflammatory, anticoagulant, and cardiovascular effects [6,7]. Most of the phytochemical studies of this plant have focused on the main bioactive compounds such as flavonoids and caffeic acid esters [8].

To further study the chemical constituents and bioactivities of *E. breviscapus*, the investigation toward its ethanol extract was conducted. Careful chromatographic purification and chemical examination led to the isolation and characterization of five new compounds, including four sesquiterpenes and one γ-pyranone glycoside. Compounds **1** and **2** were proved to be a pair of diastereomer. All the isolated compounds were tested for their neuroprotective activities against H_2O_2-induced damage in SH-SY5Y cells. Detailed information regarding the extraction, isolation, structure elucidation, and neuroprotective effects evaluation of **1–11** are reported.

2. Experimental section

2.1. General experimental procedures

The ultraviolet (UV) spectra were collected on a Shimadzu UV-1700 spectrophotometer (Kyoto, Japan). Optical rotations were measured on a JASCO DIP-370 digital polarimeter (Easton, MD, USA). CD spectra were recorded on a MOS-450 spectrometer (Bio-Logic Science Instruments, Seyssinet-Pariset, France). HRESIMS spectra were carried out on an Agilent G6520 Q-TOF spectrometer (Santa Clara, CA, USA). NMR spectra (1D and 2D NMR) were determined on Bruker ARX-300, ARX-400, and AV-600 spectrometers with trimethylsilane (TMS) as an internal standard. The chemical shifts were referenced to the residual DMSO-d_6 signal ($\delta_{C/H}$ 39.50 and 2.50) and CD_3OD-d_4 ($\delta_{C/H}$ 49.00 and

* Corresponding Author.
** Corresponding Author at: School of Traditional Chinese Materia Medica, Key Laboratory of Computational Chemistry-Based Natural Antitumor Drug Research & Development, Liaoning Province, Shenyang Pharmaceutical University, Shenyang 110016, People's Republic of China.
E-mail addresses: gpy1982@126.com (P. Gao), lilingzhijessie@163.com (L. Li), songsj99@163.com (S. Song).

https://doi.org/10.1016/j.fitote.2019.104288
Received 9 July 2019; Received in revised form 2 August 2019; Accepted 2 August 2019
Available online 06 August 2019
0367-326X/

3.31), and expressed as δ values (ppm), with coupling constants (J) reported in Hz. Column chromatography was performed on silica gel (100–200 and 200–300 mesh, Qingdao Marine Chemical Factory, Qingdao, People's Republic of China), Sephadex LH-20 gel (GE Healthcare, Sweden), polyamide-gel (80–100 mesh, Taizhou Luqiao Sijia Biochemical Plastic Factory, Zhejiang, China), MCI-gel CHP 20P (75–150 μm, Tokyo, Japan) and ODS gel (60–80 μm, Merck, Germany). TLC was carried out on precoated silica gel GF254 plates (Qingdao Marine Chemical, Inc. China). Semipreparative reversed-phase HPLC was performed on a Waters 1525 series pumping system equipped with a Waters 2489 UV detector using a YMC Pack ODS-A column (250 × 10 mm, 5 μm). Chiral HPLC isolation was run on a Shimadzu LC-10 CE liquid chromatography instrument equipped with a Shimadzu SPD-M10A UV–vis detector by using Chiralpak AD-H column (4.6 mm × 250 mm, 5 μm, Daicel Polymer Ltd., Tokyo, Japan).

2.2. Plant material

The whole plants of *E. breviscapus* were collected from Yunnan Province, People's Republic of China, in May 2016. The plant materials were identified by Professor Jincai Lu (Department of Pharmaceutical Botany, School of Traditional Chinese Materia Medica, Shenyang Pharmaceutical University, China). A voucher specimen (accession number: DZXX-2016-1Y) was maintained at the specimen room of Shenyang Pharmaceutical University.

2.3. Extraction and isolation

The air-dried aerial parts of *E. breviscapus* (20 kg) were extracted thrice with 80% EtOH at room temperature under reflux and evaporated to dryness to obtain a crude extract (4 kg). This crude extract was suspended in H_2O and successively partitioned with CH_2Cl_2 to give CH_2Cl_2-(600 g) and aqueous-soluble (3.2 kg) extracts upon evaporation in vacuo. The H_2O-soluble fraction was dissolved in MeOH and partitioned by macroporous resin column chromatography (CC) eluted with EtOH/H_2O gradient (1:1, 7:3, and 8:2, *v*/v) to give three fractions Fr.1-Fr.3. Fr.3 was fractionated by silica gel CC using CH_2Cl_2/MeOH/H_2O (9:1:0 to 1:1:0.8, v/v) to afford Fr.3.1-Fr.3.2 by TLC analysis. Fr.3.1 was separated by polyamide column (MeOH/H_2O, 6:4 to 8:2, *v*/v) followed by Sephadex LH-20 with 60% MeOH/H_2O to yield Fr.3.1.1-Fr.3.1.3. Fr.3.1.2 was further divided into three portions (Fr.3.1.2.1-Fr.3.1.2.3) by silica gel with CH_2Cl_2/MeOH, 50:1 to 1:1, v/v. Fr.3.1.2.1 and Fr.3.1.2.2 were purified by ODS column (MeOH/H_2O, 2:8 to 8:2, *v*/v) and semipreparative HPLC to obtain **10** (6.0 mg) and **11** (20.0 mg), respectively. Fr.3.1.2.3 was separated in a similar manner to Fr.3.1.2.1 to give mixed **1** and **2** (8 mg), **3** (3.5 mg), **4** (4.4 mg) and **5** (3.6 mg). Subsequently, the separation of mixed **1** and **2** by chiral HPLC using a Daicel Chiralpak AD-H chiral column eluted with *n*-hexane-isopropanol (11:1, *v*/v) detection at 210 nm afforded **1** (2.0 mg) and **2** (2.1 mg).

The dried CH_2Cl_2 extract was subjected to polyamide CC eluted with ethanol/H_2O (1:9 to 9:1, v/v) followed by MCI gel CC using aqueous ethanol to yield four fractions (Fr.1-Fr.4). Fr.1-Fr.4 were separated by using silica gel CC eluted with (CH_2Cl_2/MeOH) and purified by semi-preparative HPLC to give **6** (2.5 mg), **7** (2.2 mg), **8** (5.0 mg) and **9** (6.0 mg).

Brevisterpene A (**1**): colorless oil; ECD (MeOH) λ_{max} ($\Delta\varepsilon$) 204 (−3.30), 214 (−0.44), 245 (−0.46) nm; ^{1}H, ^{13}C NMR data (DMSO-d_6), see Tables 1 and 2; HRESIMS *m/z* 409.2181 $[M + Na]^+$ (calcd for $C_{20}H_{34}O_7$, 409.2191).

Brevisterpene B (**2**): colorless oil; ECD (MeOH) λ_{max} ($\Delta\varepsilon$) 202 (−2.99), 222 (+0.50), 243 (−0.61) nm; ^{1}H, ^{13}C NMR data (DMSO-d_6), see Tables 1 and 2; HRESIMS *m/z* 409.2181 $[M + Na]^+$ (calcd for $C_{20}H_{34}O_7$, 409.2191).

Brevisnoside A (**6**): yellow oil; $[\alpha]_D^{20}$ − 25.0 (*c* 0.10, MeOH); ^{1}H, ^{13}C NMR data (CD_3OD), see Tables 1 and 2; HRESIMS *m/z* 261.1844 $[M + Na]^+$ (calcd for $C_{15}H_{26}O_2$, 261.1825).

Brevisnoside B (**7**): yellow oil; $[\alpha]_D^{20}$ − 39.0 (*c* 0.10, MeOH); ^{1}H, ^{13}C NMR data (CD_3OD), see Tables 1 and 2; HRESIMS *m/z* 277.1778 $[M + Na]^+$ (calcd for $C_{15}H_{26}O_3$, 277.1774).

Erigeroside 6′-palmitate (**10**): white, amorphous powder; ^{1}H, ^{13}C NMR data (DMSO-d_6), see Tables 1 and 2; HRESIMS *m/z* 557.3005 $[M + COOH]^-$ (calcd for $C_{27}H_{44}O_9$, 557.2965).

2.4. Sugar analysis

2.4.1. Acid hydrolysis

Acid hydrolysis was carried out to obtain the monosaccharide of compound **10** [9]. Compound **10** (2.0 mg) was hydrolyzed with 1 M aqueous HCl (4 mL) in a thermostatically controlled oil bath at 80 °C for 4 h. After cooling, the reaction mixture was extracted with EtOAc (3 × 4 mL), and the H_2O phase was then concentrated under vacuum and dried to give a sugar residue. The residue was dissolved in H_2O (1.5 mL) and analyzed by a LCNetII/ADC HPLC with OR-4090 as the detector and equipped with a Shodex Asahipak NH2P-50 4E column using an isocratic solvent system of MeCN-H_2O (3:1, *v*/v) at a flow rate of 0.8 mL/min. The absolute configuration was determined by comparing the retention time and peak shape with standard sugar: D-glucose (t_R = 10.20 min) (Fig. S30). The sugar moiety of compound **10** was identified to be D-glucose.

2.4.2. Enzymatic hydrolysis

Compound **1** (1.0 mg) and snailase (2.0 mg) were dissolved in 3 mL of potassium dihydrogen phosphate (KDP) buffer at pH 5.6 and 37 °C for 5 h [10]. The reaction mixture was extracted with the same volume of EtOAc three times. The EtOAc extracts and water-soluble layer were evaporated to dryness in vacuum, respectively. The EtOAc extracts were purified by semi-preparative HPLC (eluted with MeCN-H_2O, 1:1, *v/v*) to afford the aglycone of **1** (0.5 mg). Compound **2** (1.1 mg) was hydrolyzed with the same procedure to afford monosaccharide. LCNetII/ADC HPLC-OR analysis showed the presence of D-glucose of **1** and **2** (Fig. S30).

2.5. ECD calculations

The absolute configurations of the aglycone of **1** and **2** were determined by using time-dependent density functional theory (TDDFT) calculations. Conformational distribution of the optimized structures was investigated at B3LYP/6-31G(d) and suggested the major conformers (> 98%). Energies of the geometric conformations in MeOH were calculated at the B3LYP/6–311 + G(d) level. The hybrid B3LYP functions were chose to run the TDDFT calculations, solving for 25 states for per molecule. The ECD of the conformers were performed by the TDDFT method at the B3LYP/6-31G(d) level with the CPCM model in methanol solution, and the overall ECD curves were produced by SpecDis 1.51 [11–13].

2.6. Optical rotation calculations

A conformational search using the Molecular Merck force field (MMFF) led to the identification of the major conformers (> 95%), which was performed using the Gaussian 09 program at B3LYP/6-31G(d) level [14]. Geometry optimization followed by OR calculations at D-sodium line radiation (wavelength of 589 nm) in MeOH (CPCM) using the B3LYP functional and the 6–311 + + G(2d,p) basis set for DFT. Final calculated ORs were obtained as the result of the Boltzmann-weighted average.

2.7. ^{13}C NMR calculations

After optimization of the major conformers (> 95%) was performed using the Gaussian 09 program at B3LYP/6-31G(d) level. Computed chemical shifts reported in this study were determined using the GIAO

Table 1
^{1}H (600 MHz) NMR spectroscopic data for compounds **1**, **2**, **6**, **7** and **10**.

No.	1[a]	2[a]	6[b]	7[b]	10[a]
1			4.13 (2H, m)	4.02 (1H, overlapped)	
2	1.40 (1H, t, 12.2)	1.40 (1H, t, 12.2)	5.54 (1H, t, 6.4)	5.61 (1H, s)	8.12 (1H, s)
	1.80 (1H, m)	1.79 (1H, m)			
3	3.97 (1H, m)	3.96 (1H, m)			
4	1.95 (1H, dd, 17.0, 9.6)	1.96 (1H, dd, 16.8, 9.6)	3.95 (1H, t, 6.8)	3.93 (1H, overlapped)	
	2.39 (1H, m)	2.39 (1H, dd, 16.8, 5.8)			
5			2.25 (2H, t, 6.9)	1.70 (2H, m)	6.40 (1H, d, 5.6)
6			5.12 (1H, overlapped)	1.42 (1H, m)	8.13 (1H, d, 5.9)
7	5.99 (1H, d, 15.9)	5.99 (1H, d, 15.9)		2.01 (1H, m)	
8	5.22 (1H, dd, 15.9, 7.9)	5.23 (1H, d, 15.9, 7.8)	1.99 (2H, t, 7.5)	1.34 (2H, m)	
9	3.76 (1H, m)	3.76 (1H, p, 6.6)	2.07 (2H, t, 7.5)	2.09 (2H, m)	
10	1.17 (3H, d, 6.3)	1.18 (3H, d, 6.3)	5.09 (1H, overlapped)	5.14 (1H, t, 7.3)	
11	3.18 (3H, s)	3.18 (3H, s)			
12	1.02 (3H, s)	1.00 (3H, s)	1.67 (3H, s)	1.67 (3H, s)	
13	0.99 (3H, s)	0.99 (3H, s)	1.60 (3H, s)	1.61 (3H, s)	
14	1.66 (3H, s)	1.67 (3H, s)	1.62 (3H, s)	3.93 (1H, overlapped)	
				4.00 (1H, overlapped)	
15			1.64 (3H, s)	0.82 (3H, d, 6.9)	
1′	4.28 (1H, d, 7.8)	4.28 (1H, d, 7.8)			4.85 (1H, d, 7.0)
2′	3.13 (1H, m)	3.11 (1H, m)			3.20 (1H, m)
3′	2.91 (1H, m)	2.90 (1H, m)			3.21 (1H, m)
4′	3.04 (1H, m)	3.04 (1H, m)			3.11 (1H,m)
5′	3.09 (1H, m)	3.08 (1H, m)			3.54 (1H, m)
6′	3.44 (1H, dt, 11.6, 5.8)	3.43 (1H, dt, 11.7, 5.9)			4.04 (1H, dd, 11.9, 6.8)
	3.65 (1H, m)	3.65 (1H, m)			4.28 (1H, d, 11.8)
Glc-OH	4.44 (1H, t, 5.8)	4.46 (1H, t, 5.8)			5.47 (1H, d, 4.9)
Glc-OH	4.95 (1H, d, 4.7)	4.94 (1H, d, 4.7)			5.22 (1H, d, 4.8)
Glc-OH	4.90 (2H, d, 4.9)	4.91 (2H, dd, 8.3, 4.9)			5.29 (1H, d, 5.5)
1″					
2″					2.26 (2H, m)
3″					1.49 (2H, m)
4″-15″					1.22 (24H, m)
16″					0.85 (3H, t, 6.9)

[a] Recorded in DMSO-d6.
[b] Recorded in methanol-d_4.

method in Gaussian 09 at the B3LYP/6–311 + + G(2d,p) level of theory [15]. The scaled calculated ^{13}C NMR chemical shifts were obtained from the following: $\delta_{scal.calc.} = (\delta_{calc.} - \text{intercept})/\text{slope}$. A result was evaluated in terms of R^2, MaxDev and AveDev (Table S5). Among them, R^2 is its coefficient of determination. MaxDev is the maximum absolute deviation with respect to the experimental chemical shifts δ_{exp}. AveDev is the average absolute deviation, computed as $(1/n)\ \Sigma_{i=1}^{n} |\delta_{scale.calc.} - \delta_{exp.}|$.

2.8. Neuroprotective activity assay

The neuroprotective activities of all isolated compounds (**1**−**11**) toward H_2O_2-induced SH-SY5Y cells damaged by the MTT assay were screened following the reported procedures [16].

3. Results and discussion

Brevisterpene A (**1**) was isolated as yellow oil and found to have a molecular formula of $C_{20}H_{34}O_7$, based on the HRESIMS ion peak at *m/z* 409.2181 $[M + Na]^+$ and its ^{13}C NMR data, accounting for four indices of hydrogen deficiency. The ^{1}H NMR data (DMSO-d_6, Table 1) exhibited resonances assignable to two olefinic protons (δ_H 5.99, d, J = 15.9 Hz, H-7; δ_H 5.22, dd, J = 15.9, 7.9 Hz, H-8), one methoxyl (δ_H 3.18, s, CH_3-11), an oxymethine (δ_H 3.97, m, H-3), four methyl groups (δ_H 1.17, d, J = 6.3 Hz, CH_3-10; 1.02, s, CH_3-12; 0.99, s, CH_3-13; 1.66, s, CH_3-14). The presence of a sugar moiety was shown by the appearance of an anomeric proton doublet at δ_H 4.28 (1H, d, J = 7.8 Hz, H-1′), which correlated to its anomeric carbon signal at δ_C 100.7 (C-1′) in the HMQC spectrum, and four oxygenated methines and an oxygenated methylene. Correspondingly, analysis of the ^{13}C NMR data and HSQC spectra indicated that **1** contained four olefinic carbons (δ_C 125.5, C-5; 136.4, C-6; 128.4, C-7; 136.1, C-8), one *O*-methyl groups (δ_C 55.2, C-11), four methyl groups (δ_C 21.6, C-10; 21.1, C-14; 28.1, C-12; 29.9, C-13), two oxymethine carbons (δ_C 70.0, C-3; 77.6; C-9), two methine groups (δ_C 45.6, C-2; 38.5, C-4), a quaternary carbon (δ_C 36.1, C-1), and one glucose moiety carbon signal (δ_C 100.7, C-1′; 76.8, C-2′; 73.5, C-3′; 70.1, C-4′; 76.7, C-5′; 61.1, C-6′) (Table 2). Based on detailed analyses of 2D NMR data, the planar structure of **1** was constructed in Fig. 1. The HMBC correlations from H-2 to C-1 (δ_C 36.1), C-3 (δ_C 70.0), and C-4 (δ_C 38.5) and from H-4 to C-2 (δ_C 45.6), C-3 (δ_C 70.0), C-5 (δ_C 125.5), and C-6 (δ_C 136.4) confirmed the presence of an unsaturated six-membered ring. Correlations from CH_3-12 and CH_3-13 to C-1 (δ_C 36.1), C-2 (δ_C 45.6), and C-6 (δ_C 136.4) indicated the attachment of two methyl groups at C-1. HMBC correlations from CH_3-10 to C-8 (δ_C 136.1), and C-9 (δ_C 77.6) and CH_3-14 to C-4 (δ_C 38.4), C-5 (δ_C 125.5), and C-6 (δ_C 136.4) justified the assignment of two methyl groups to C-5 and C-9, respectively. The double bond at C-7/C-8 was also joined at C-6 and C-9 on the basis of correlations from H-7 to C-5 (δ_C 125.5) and C-9 (δ_C 77.6) and H-8 to C-6 (δ_C 136.4) and C-9 (δ_C 77.6). The HMBC correlation of the signal at δ_H 3.18 with C-9 (δ_C 77.6) placed methoxy group on C-9.

Due to two separated resonances at some of the carbons (Fig. S28), compounds **1** and **2** were proved to be a pair of mixed sesquiterpenes, and it was presented as a single peak in the HPLC using both the C18 or silica gel columns. Mixed compounds **1** and **2** were separated using a chiral AD-H column eluted with *n*-hexane-isopropanol to successfully obtain pure compounds **1** and **2** (Fig. S29). The molecular formula of

Table 2
^{13}C (100 MHz) NMR spectroscopic data for compounds **1**, **2**, **6**, **7** and **10**.

No.	1[a]	2[a]	6[b]	7[b]	10[a]
1	36.1	36.1	59.2	69.4	
2	45.6	45.6	126.2	127.4	144.0
3	70.0	70.0	140.6	141.0	145.7
4	38.5	38.5	78.1	66.5	172.3
5	125.5	125.5	34.7	21.9	116.2
6	136.4	136.4	121.7	47.4	155.7
7	128.4	128.3	137.8	32.0	
8	136.1	136.2	40.9	36.7	
9	77.6	77.6	27.8	27.0	
10	21.6	21.6	125.4	125.9	
11	55.2	55.2	132.1	131.9	
12	28.1	28.0	25.9	25.9	
13	29.9	30.0	17.7	17.7	
14	21.1	21.1	11.8	66.5	
15			16.4	14.5	
1′	100.7	100.7			99.9
2′	76.8	76.8			73.0
3′	73.5	73.5			76.3
4′	70.1	70.1			69.7
5′	76.7	76.8			73.8
6′	61.1	61.1			63.1
1″					172.7
2″					33.5
3″					24.4
4″					28.4
5″-13″					29.0
14″					22.1
15″					31.3
16″					13.9

[a] Recorded in DMSO-d_6.
[b] Recorded in methanol-d_4.

brevisterpene B (**2**) was deduced as $C_{20}H_{34}O_7$ from the HRESIMS and ^{13}C NMR spectroscopy, the same as **1**. Careful comparison of all the NMR spectra involving the ^{1}H, ^{13}C, and 2D-NMR values of **1** and **2** revealed that these compounds have an identical planar structure. The *E* configuration of the 7,8-diene was deduced from the coupling constant ($J_{7,8}$ = 15.9 Hz). According to the large coupling constant of the anomeric proton at δ_H 4.28 (J = 7.8 Hz, H-1′), the orientation of glucose moiety was deduced to be β-configuration. The glycosidation at C-3 was determined by a long-range correlation between δ_H 4.28 (H-1′) and δ_C 70.0 (C-3) in the HMBC spectra of **1** and **2**. The D configuration of sugar portion of **1** and **2** were confirmed by the analysis of LCNetII/ADC HPLC-OR [9,10] (Fig. S30).

However, the NOESY correlations could not provide sufficient information to elucidate the unambiguous relative configuration of C-3 and C-9. The absolute configuration of C-3 and C-9 asymmetric center in the aglycone of **1** and **2** were established by time-dependent Density Function Theory (TDDFT) calculations of the electronic circular dichroism (ECD) spectrum. Quantum chemical calculations were conducted for the (3*S*, 9*S*) and (3*R*, 9*R*), (3*R*, 9*S*) and (3*S*, 9*R*) isomers of the aglycone of **1** and **2** using TDDFT at the B3LYP/6-31G (d) level with CPCM in methanol, and the experimental ECD spectrum of the aglycone of **1** matched well with the calculated ECD spectrum of **1a** (Fig. 3). And, the experimental ECD spectrum of the aglycone of **2** matched well with the calculated ECD spectrum of **2a** (Fig. 3). Thus, the absolute configurations of the aglycone of **1** and **2** were determined as 3*S*, 9*S* and 3*S*, 9*R*, respectively. Compounds **1** and **2** were proved to be a pair of diastereomer.

The molecular formula of brevisnoside A (**6**) was established as $C_{15}H_{26}O_2$ according to the $[M + Na]^+$ ion peak at *m/z* 261.1844 in the (+) HRESIMS spectrum with an index of three hydrogen deficiency.

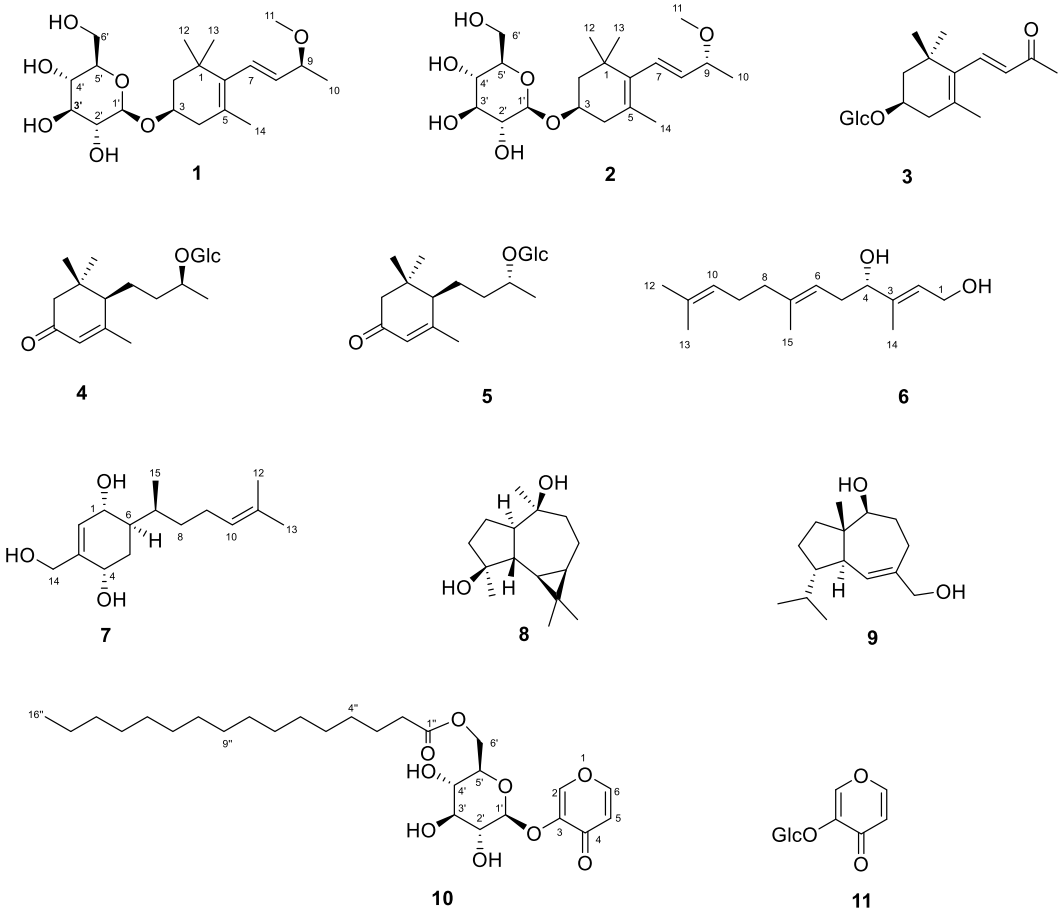

Fig. 1. The structures of compounds **1–11**.

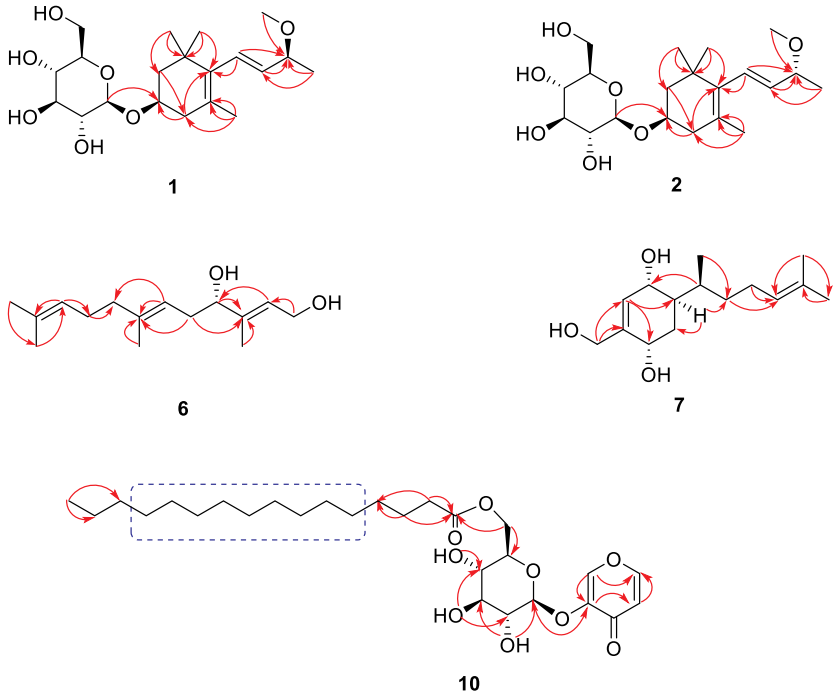

Fig. 2. Key HMBC correlations of compounds **1**, **2**, **6**, **7** and **10**.

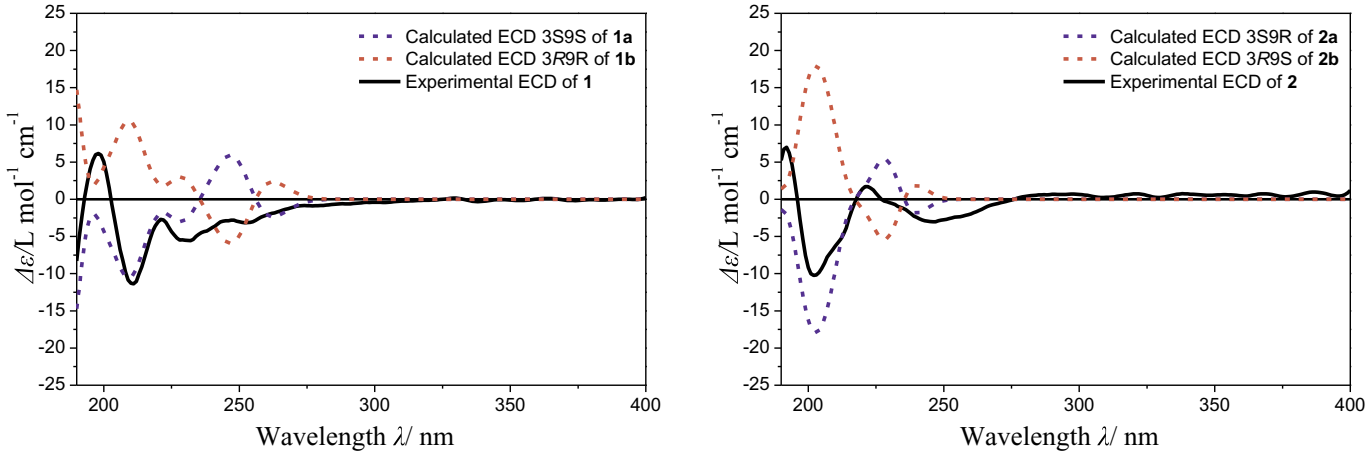

Fig. 3. Electronic circular dichroism (ECD) spectra of compounds **1** and **2** recorded in methanol in the 400–200 nm range. Calculated ECD spectra were shown in red and blue compared to the experimental values shown in black. (For interpretation of the references to colour in this figure legend, the reader is referred to the web version of this article.)

The ^{1}H, ^{13}C NMR data (Tables 1 and 2) and HSQC analysis of **6** indicated the presence of six olefinic carbons (three are proton-bearing), four methyls, an oxygenated methenyl, one oxygenated methylene, and three methylenes. In the HMBC spectrum, the correlations between CH_3-12/CH_3-13 to C-10 (δ_C 125.4)/C-11 (δ_C 132.1), CH_3-15 to C-6 (δ_C 121.7)/C-7 (δ_C 137.8)/C-8 (δ_C 40.9), and CH_3-14 to C-2 (δ_C 126.2)/C-3 (δ_C 140.6)/C-4 (δ_C 78.1) were observed. The HMBC correlations of H-1 to C-2 (δ_C 126.2)/C-3 (δ_C 140.6), H-2 to C-4 (δ_C 78.1), H-6 to C-5 (δ_C 34.7)/C-7 (δ_C 137.8)/C-8 (δ_C 40.9), H-9 to C-7 (δ_C 137.8), and H-10 to C-9 (δ_C 27.8)/C-11 (δ_C 132.1) suggested the planer structure of **6** (Fig. 2). In addition, the NOESY correlations of H-14 with H-1 and H-5, H-15 with H-5 and H-9 suggested that the double bonds at C-6/7 and C-2/3 are both *E* configuration, respectively (Fig. 4).

The absolute configuration of **6** was established by comparison of the experimental and calculated OR value [16]. A conformational search using the MMFFs force field for the (4*S*)-stereoisomer and its enantiomer led to the identification of 32 conformers, followed by geometric optimization of each one. The optimized conformers were subjected to OR calculations in MeOH (CPCM) using the B3LYP functional and the 6–311 + G(d) basis set for DFT. Final calculated ORs were obtained as the result of the Boltzmann-weighted average (Table S4). From these results, the negative calculated ORs ($[\alpha]_D^{20}$ − 26.6) of the (4*S*)-stereoisomer was a better fit to the experimental OR value ($[\alpha]_D^{20}$ − 25.0, *c* 0.1, MeOH) than the positive one ($[\alpha]_D^{20}$ + 26.6). Therefore, the structure of **6** was identified as shown.

Brevisnoside B (**7**), having a molecular formula of $C_{15}H_{26}O_3$ (*m/z* 277.1778 $[M + Na]^+$), was also obtained as a yellow oil. Its ^{1}H, ^{13}C NMR and HSQC spectra showed characteristic resonances of two double bonds, three methyls, four methylenes (including one oxygenated), one methine and two oxygenated methines groups (Tables 1 and 2). The key HMBC correlations from CH_3-13 to C-10 (δ_C 125.9), C-11 (δ_C 131.9), and C-12 (δ_C 25.9); from CH_3-12 to C-10 (δ_C 125.9), C-11 (δ_C 131.9), and C-13 (δ_C 17.7); from CH_3-15 to C-6 (δ_C 47.4), C-7 (δ_C 32.0), and C-8 (δ_C 36.7); from H-9 to C-7 (δ_C 32.0), C-8 (δ_C 36.7), C-10 (δ_C 125.9), and

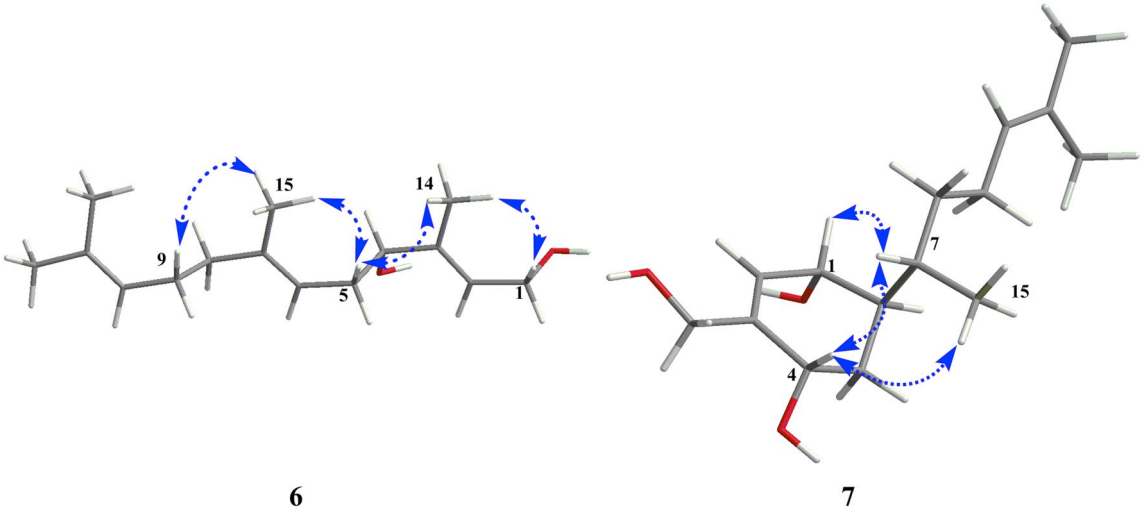

Fig. 4. Selected NOESY correlations of **6** and **7**.

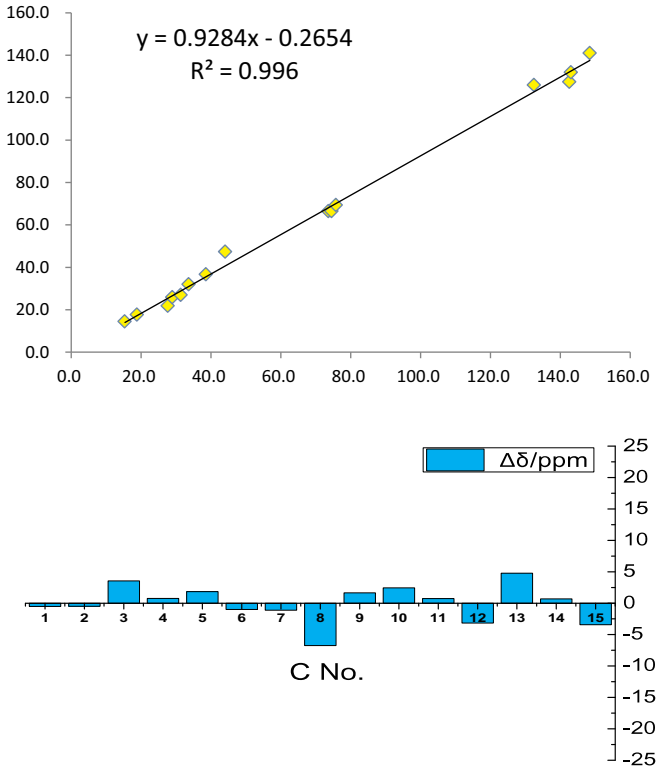

Fig. 5. Experimental and calculated ^{13}C chemical shifts of **7**.

C-11 (δ_C 131.9) confirmed the presence of a $(CH_3)_2C=CHCH_2CH_2(CH_3)$- group. The six-membered ring moiety was further elaborated via the HMBC correlations from H-2 to C-4 (δ_C 66.5) and C-6 (δ_C 47.4), and from H-6 to C-5 (δ_C 21.9) and C-8 (δ_C 36.7). Additionally, a hydroxymethyl group was attached at C-3 according to the HMBC correlations from H-12 to C-2 (δ_C 127.4) and C-3 (δ_C 141.0). Thus, the planar structure of **7** was elucidated as a bisabolene-type sesquiterpene.

The relative configuration of **7** was determined by the analysis of NOESY spectrum in Fig. 4. The NOESY correlations of H-1/H-7, H-4/H-7 and H-4/CH_3-15 indicated their co-facial orientation, which were arbitrarily assigned as *β*. However, the orientation of H-6 were assigned as *α*. In addition, the relative configuration at C-7 was established by calculated ^{13}C NMR [17,18]. High-accuracy ^{13}C NMR calculation of two possible stereoisomers (1*R**, 4*S**, 6*R**, 7*R** or 1*R**, 4*S**, 6*R**, 7*S**) indicated that the potential one is 1*R**, 4*S**, 6*R**, 7*S** (R^2 = 0.9960, AveDev = 2.2) better than 1*R**, 4*S**, 6*R**, 7*R** (R^2 = 0.9953, AveDev = 2.4) (Fig. 5, Table S5).

The absolute configuration of **7** was established by comparison of the experimental and calculated OR value []. Due to the above NMR data, the configuration of **7** was identified as one of the two isomers (1*R*, 4*S*, 6*R*, 7*S* or 1*S*, 4*R*, 6*S*, 7*R*). A conformational search using the MMFFs force field for the (1*R*, 4*S*, 6*R*, 7*S*)-stereoisomer and its enantiomer led to the identification of 17 conformers, followed by geometric optimization of each one. The optimized conformers were subjected to OR calculations in MeOH (CPCM) using the B3LYP functional and the 6–311 + + g(2d,p) basis set for DFT. Final calculated ORs were obtained as the result of the Boltzmann-weighted average (Table S4). From these results, the negative calculated ORs ($[\alpha]_D^{20}$ − 13.0) of the (1*R*, 4*S*, 6*R*, 7*S*)-stereoisomer was a better fit to the experimental OR value ($[\alpha]_D^{20}$ − 39.0, *c* 0.1, MeOH) than the positive one ($[\alpha]_D^{20}$ + 13.0). Therefore, the structure of **7** was identified as shown.

Erigeroside 6′-palmitate (**10**) was obtained as an amorphous, white solid. It has the molecular formula $C_{27}H_{44}O_9$ as deduced from HRESIMS data with a negative ion peak at *m/z* 557.3005 $[M + COOH]^-$, corresponding to six indices of hydrogen deficiency. The ^{1}H NMR data of **10** (Table 1) revealed three olefinic signals at δ_H 8.13 (1H, d, *J* = 5.9 Hz, H-6), 8.12 (1H, s, H-2), and 6.40 (1H, d, *J* = 5.6 Hz, H-5). A characteristic *β*-glucopyranosyl unit was evidenced at δ_H 4.85 (1H, d, *J* = 7.0 Hz, H-1′), 3.20 (1H, m, H-2′), 3.21 (1H, m, H-3′), 3.11 (1H, m, H-4′), 3.54 (1H, m, H-5′), 4.29 (1H, d, *J* = 11.8 Hz, H-6′a), and 4.04 (1H, dd, *J* = 11.9 Hz, 6.8 Hz, H-6′b), and the exchangeable protons of δ_H 5.47, 5.22, and 5.29 were assigned in this hexose ring based on the HSQC and HMBC correlations (Fig. 2). In addition, the characteristic signals at δ_H 0.85 (3H, t, *J* = 6.9 Hz, H-16″) and 1.22 (24H, m, from H-5″ to H-13″) indicated the presence of a long alkyl chain. The HRESIMS, ^{13}C NMR data, and HSQC spectrum of **7** revealed the presence of 27 carbon signals, comprising four olefinic carbons (δ_C 144.0, C-2; 145.7, C-3; 116.2, C-5; 155.7, C-6), two carbonyl carbons (δ_C 172.3 C-4; 172.7, C-1″), a *β*-glucopyranosyl unit (δ_C 99.9, C-1′; 73.0, C-2′; 76.3, C-3′; 69.7, C-4′; 73.8, C-5′; 63.1, C-6′), 14 nonoxygenated methylenes (from δ_C 22.1 to 33.5, C-2″-C-15″), and one terminal methyl (δ_C 13.9, C-16″) (Table 2).

The structure of **10** was determined mainly by using 2D data (Fig. 2). The HMBC spectrum of **10** showed correlations of H-2, H-5/C-3 (δ_C 145.7), C-6 (δ_C 155.7), H-6/C-2 (δ_C 144.0), C-4 (δ_C 172.3), C-5 (δ_C 116.2), indicating that the existence of a γ-pyrone ring. Correlations of H-2″/C-1″ (δ_C 172.7), C-3″ (δ_C 24.4), C-4″ (δ_C 28.4), H-3″/C-1″ (δ_C 172.7), C-2″ (δ_C 33.5), C-4″ (δ_C 28.4), and CH_3-16″/C-14″ (δ_C 22.1), C-

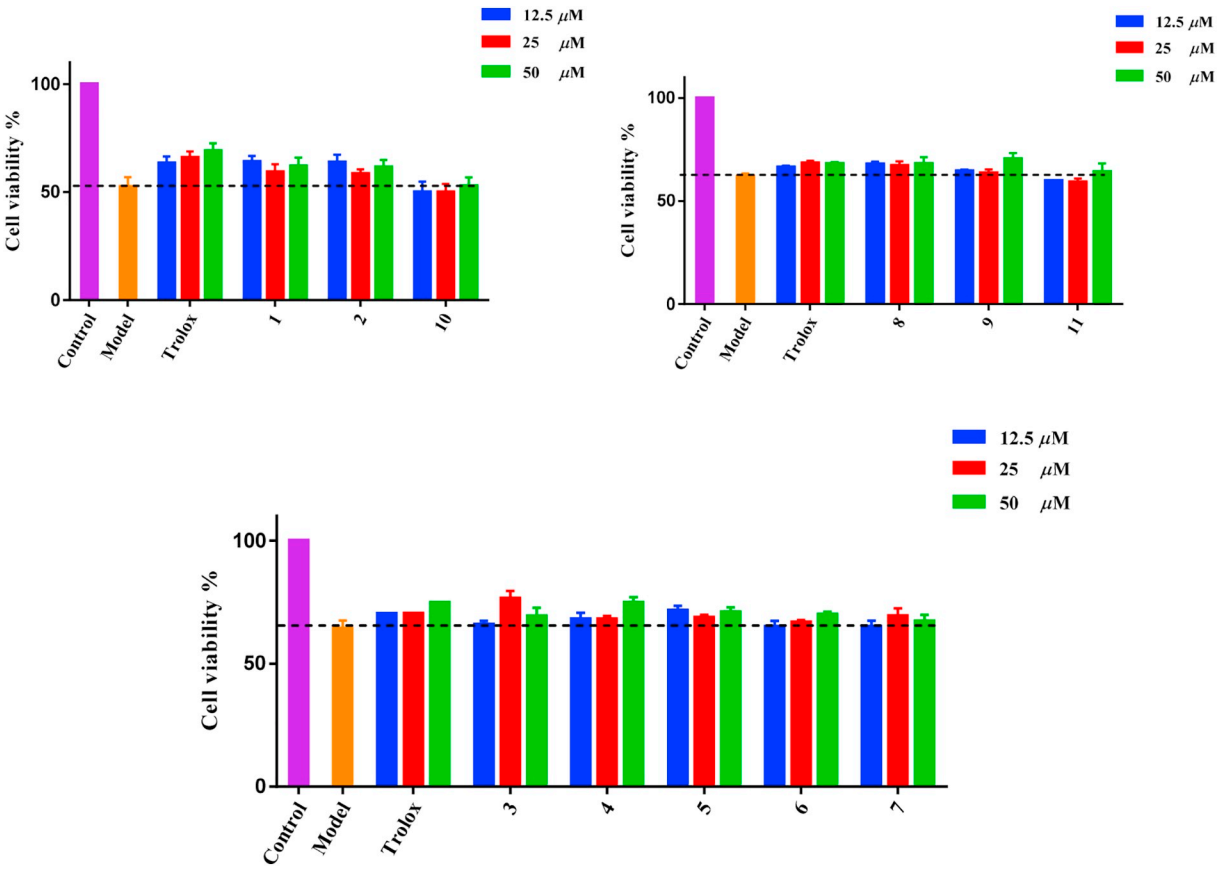

Fig. 6. The neuroprotective effects of compounds **1–11** against H_2O_2-induced injury of SH-SY5Y cells. MTT assay was used to determine the cell viability in the presence or absence of the tested compounds at different concentrations (12.5, 25.0, 50.0 μM).

15″ (δ_C 31.3) revealed the partial structure of an alkyl hydrophobic chain starting from the carbonyl (C-1″) group. A key correlation from H-1′ to C-3 (δ_C 145.7) indicated that the glucosyl moiety was located to C-3. The correlations from H-6′ to C-5′ (δ_C 73.8) and C-1″ (δ_C 172.7) established a bridge between a hexose ring and an alkyl chain. Acid hydrolysis of **10** afforded D-glucose, as determined by LCNetII/ADC HPLC-OR analysis (Fig. S30).

Known compounds 3*β*-glucopyranosyloxy-*β*-ionone (**3**) [19], blumenol C glucoside (**4**) [20], byzantionoside B (**5**) [20], 4*β*,10*β*-aromadendranediol (**8**) [21], 4-epi-isodauc-6-ene-10*β*,14-diol (**9**) [22], and erigeroside (**11**) [23] were identified by comparing their experimental and reported spectroscopic data.

All compounds (**1–11**) were tested for neuroprotective effects against H_2O_2-induced damage in human neuroblastoma SH-SY5Y cells at the concentration of 12.5, 25.0 and 50.0 μm, with Trolox used as a positive control, using a MTT assay (Fig. 6) [16]. As a result, compounds **1** and **2** had moderate neuroprotective effects at concentrations of 12.5 and 50.0 μM, which improved cell viabilities by > 10% compared with the model group (Table S1). Compounds **3** and **4** had weak neuroprotective effects. Furthermore, compounds **10** and **11** with pyrone glycosides exhibited no neuroprotective effects at the tested concentrations.

4. Conclusion

In summary, five novel metabolites including two sesquiterpenoid glycosides (**1–2**), two sesquiterpenes (**6–7**) and one pyranone glycoside (**10**) were obtained from the whole plant of *E. breviscapus*. Compounds **1** and **2** were a pair of diastereomer separated by chiral-phase column chromatography. All compounds (**1–11**) were evaluated for their neuroprotective activities *in vitro*, and compounds **1** and **2** showed moderate effects against H_2O_2-induced injury in SH-SY5Y cells at the concentration of 12.5 and 25.0 μm.

Declaration of Competing Interest

The authors declare no conflict of interest.

Acknowledgments

This study was financially supported by the National Nature Science Foundation (81673324) of the People's Republic of China and the innovative experiment projects of undergraduate (201910163113) of Shenyang Pharmaceutical University.

Appendix A. Supplementary data

Supplementary data to this article can be found online at https://doi.org/10.1016/j.fitote.2019.104288.

References

[1] J. Yang, G.H. Zhang, J. Zhang, H. Liu, W. Chen, X. Wang, Y.H. Li, Y. Dong, S.H. Yang, Hybrid de novo genome assembly of the Chinese herbal fleabane *Erigeron breviscapus*, GigaScience 6 (2017), https://doi.org/10.1093/gigascience/gix028.
[2] J.L. Gao, G. Chen, H.Q. He, C. Liu, X.J. Xiong, J. Li, J. Wang, Therapeutic effects of breviscapine in cardiovascular diseases: a review, Front. Pharmacol. 8 (2017), https://doi.org/10.3389/fphar.2017.00289.
[3] J. Qu, Y.M. Wang, G.A. Luo, Z.P. Wu, Identification and determination of glucuronides and their aglycones in *Erigeron breviscapus* by liquid chromatography-tandem mass spectrometry, J. Chromatogr. A 928 (2001) 155–162, https://doi.org/10.1016/s0021-9673(01)01111-6.
[4] X. Li, K.X. Song, J.B. Yang, T.S. Yi, Isolation and characterization of 11 new microsatellite loci in *Erigeron breviscapus* (Asteraceae), an important Chinese traditional herb, Int. J. Mol. Sci. 12 (2011) 7265–7270, https://doi.org/10.3390/

ijms12107265.
[5] H. Sun, A drug for treating cardio-cerebrovascular diseases-phenolic compounds of *Erigeron breviscapus*, Prog. Chem. 21 (2009) 77–83.
[6] M. Karamese, H.S. Erol, M. Albayrak, G. Findik Guvendi, E. Aydin, S. Aksak Karamese, Anti-oxidant and anti-inflammatory effects of apigenin in a rat model of sepsis: an immunological, biochemical, and histopathological study, Immunopharmacol. Immunotoxicol. 38 (2016) 228–237, https://doi.org/10.3109/08923973.2016.1173058.
[7] Q.C. Chu, T. Wu, L. Fu, J.N. Ye, Simultaneous determination of active ingredients in *Erigeron breviscapus* (Vant.) Hand-Mazz. by capillary electrophoresis with electrochemical detection, J. Pharmaceut. Biomed. 37 (2005) 535–541, https://doi.org/10.1016/j.jpba.2004.11.018.
[8] S.Y. Chen, M. Li, Y.T. Li, H.J. Hu, Y. Li, Y. Huang, Y. Zheng, Y. Lu, J. Hu, Y.Y. Lan, A.M. Wang, Y.J. Li, Z.P. Gong, Y.L. Wang, A UPLC-ESI-MS/MS method for simultaneous quantitation of chlorogenic acid, scutellarin, and scutellarein in rat plasma: application to a comparative pharmacokinetic study in sham-operated and MCAO rats after oral administration of *Erigeron breviscapus* extract, Molecules 23 (2018) 1808, https://doi.org/10.3390/molecules23071808.
[9] W.Y. Zhao, X.Y. Song, L. Zhao, C.X. Zou, W.Y. Zhou, B. Lin, G.D. Yao, X.X. Huang, S.J. Song, Quassinoids from *Picrasma quassioides* and their neuroprotective effects, J. Nat. Prod. 82 (2019) 714–723, https://doi.org/10.1021/acs.jnatprod.8b00470.
[10] C. Zhang, J. Li, J. Wang, X.L. Song, J. Zhang, S. Wu, J.J. Zhang, S. Wu, C.L. Hu, Z.Y. Gong, L. Jia, Antihyperlipidaemic and hepatoprotective activities of acidic and enzymatic hydrolysis exopolysaccharides from Pleurotus eryngii SI-04, BMC Complem. Altern. M. 17 (2017) 403, https://doi.org/10.1186/s12906-017-1892-z.
[11] J. Bulusu, R. Surasani Sumathi, R.P. Thangavelu, Conformational preferences of 1,4,7-trithiacyclononane: a molecular mechanics and density functional theory study, J. Mol. Model. 10 (2004) 55–59, https://doi.org/10.1007/s00894-003-0166-5.
[12] H. Goto, E. Osawa, Corner flapping: a simple and fast algorithm for exhaustive generation of ring conformations, J. Am. Chem. Soc. 111 (1989) 8950–8951, https://doi.org/10.1021/ja0020 (6a046).
[13] T. Bruhn, A. Schaumlöffel, Y. Hemberger, G. Bringmann, SpecDis: quantifying the comparison of calculated and experimental electronic circular dichroism spectra, Chirality. 25 (2013) 243–249, https://doi.org/10.1002/chir.22138.
[14] T. Yanai, D.P. Tew, N.C. Handy, A new hybrid exchange-correlation functional using the coulomb-attenuating method (CAM-B3LYP), Chem. Phys. Lett. 393 (2004) 51–57, https://doi.org/10.1016/j.cplett.2004.06.011.
[15] X.W. Hou, S. Han, Y.Y. Zhang, H.B. Su, P.Y. Gao, L.Z. Li, S.J. Song, Neogenkwanine I from the flower buds of *Daphne genkwa* with its stereostructure confirmation using quantum calculation profiles and antitumor evaluation, Nat. Prod. Res. (2018) 1–8, https://doi.org/10.1080/14786419.2018.1536133.
[16] Q. Ren, W.Y. Zhao, S.C. Shi, F.Y. Han, Y.Y. Zhang, Q.B. Liu, G.D. Yao, B. Lin, X.X. Huang, S.J. Song, Guaiane-type sesquiterpenoids from the roots of *Daphne genkwa* and evaluation of their neuroprotective effects, J. Nat. Prod. 82 (2019) 1510–1517, https://doi.org/10.1021/acs.jnatprod.8b01049.
[17] Y. Tang, Y.B. Xue, G. Du, J.P. Wang, J.J. Liu, B. Sun, X.N. Li, G.M. Yao, Z.W. Luo, Y.H. Zhang, Structural revisions of a class of natural products: scaffolds of aglycon analogues of fusicoccins and cotylenins isolated from fungi, Angew. Chem. 128 (2016) 4137–4141, https://doi.org/10.1002/ange.201600313.
[18] C.Y. Zhang, L. Luo, J. Xia, Y.N. Song, L.J. Zhang, M. Zhang, K. Rahman, Y. Ye, H. Zhang, J.Y. Zhu, Sesquiterpenes and lignans from the flower buds of Daphne genkwa and their nitric oxide inhibitory activities, Nat. Prod. Res. (2017) 1–7, https://doi.org/10.1080/14786419.2017.1389937.
[19] A. Fiorentino, B. D'Abrosca, S. Pacifico, C. Mastellone, V. Piscopo, P. Monaco, Spectroscopic identification and antioxidant activity of glucosylated carotenoid metabolites from *Cydonia vulgaris Fruits*, J. Agric. Food Chem. 54 (2006) 9592–9597, https://doi.org/10.1021/jf062125e.
[20] K. M atsunami, H. Otsuka, Y. Takeda, Structural revisions of blumenol C glucoside and byzantionoside B, Chem. Pharm. Bull. 58 (2010) 438–441, https://doi.org/10.1248/cpb.58.438.
[21] I.C. Moreira, J.H.G. Lago, M.C.M. Young, N.F. Roque, Antifungal aromadendrane sesquiterpenoids from the leaves of *Xylopia brasiliensis*, J. Braz. Chem. Soc. 14 (2003) 828–831, https://doi.org/10.1590/s0103-50532003000500020.
[22] X.M. Zhou, C.J. Zheng, Y.Q. Zhang, X.P. Zhang, X.P. Song, W. Xu, G.Y. Chen, Guaiane-type sesquiterpenoids from *Fissistigma oldhamii* inhibit the proliferation of synoviocytes, Planta Med. 83 (2016) 217–223, https://doi.org/10.1055/s-0042-111440.
[23] M. Tafazzoli, M. Ghiasi, M. Moridi, Dynamic stereochemistry of erigeroside by measurement of ^{1}H-^{1}H and ^{13}C-^{1}H coupling constants, Spectrochim. Acta A 70 (2008) 350–357, https://doi.org/10.1016/j.saa.2007.10.033.